

Probing omics data via harmonic persistent homology *

Davide Gurnari^{1†}[0000-0002-3668-8711], Aldo Guzmán-Sáenz^{2†}[0000-0003-2725-621X], Filippo Utró²[0000-0003-3226-7642], Aritra Bose²[0000-0002-8665-056X], Saugata Basu³[0000-0002-2441-0915], and Laxmi Parida²[0000-0002-7872-5074]

¹ Dioscuri Centre in Topological Data Analysis, Mathematical Institute PAN, Warsaw, PL

² IBM Research, Yorktown Heights, NY, USA

³ Dept. of Mathematics, Purdue University, West Lafayette, IN, USA

parida@us.ibm.com

Abstract. Identifying molecular signatures from complex disease patients with underlying symptomatic similarities is a significant challenge in the analysis of high dimensional multi-omics data. Topological data analysis (TDA) provides a way of extracting such information from the geometric structure of the data and identifying multiway higher-order relationships. Here, we propose an application of *Harmonic* persistent homology, which overcomes the limitations of ambiguous assignment of the topological information to the original elements in a representative topological cycle from the data. When applied to multi-omics data, this leads to the discovery of hidden patterns highlighting the relationships between different omic profiles, while allowing for common tasks in multi-omics analyses, such as disease subtyping, and most importantly biomarker identification for similar latent biological pathways that are associated with complex diseases. Our experiments on multiple cancer data show that *harmonic* persistent homology effectively dissects multi-omics data to identify biomarkers by detecting representative cycles predictive of disease subtypes.

Keywords: Topological Data Analysis · Pattern Discovery · Data Analysis

1 Introduction

Omics studies have gained substantial importance in unraveling interactions between biomarkers that underlie complex diseases given the increasing availability of such data from across modalities due to recent technological advances [8]. These biomarkers are instrumental in clinical decision-making and drug discovery. However, extracting them from complex data can often be a challenge with the high dimensionality of these datasets as well as the heterogeneous molecular profiles of patients, disease subtypes, and other biases that plague epidemiological studies [12]. Furthermore, identifying biomarkers that share similar underlying biological pathways or molecular profiles among patients can be an even bigger impediment that still need investigation and novel analytical tools. One of the most robust approaches that analyzes data with a new perspective is Topological Data Analysis (TDA). TDA has been shown as a useful tool for the analysis of omics data [3,5,10,22,20,16,15,19,13,21], and it enables the identification of (complex) multiway high order relationships in the data.

Persistent homology is a tool from TDA used to study the topology of spaces at different scales with algebraic constructs. This approach has been used successfully in the context of pattern discovery (see for example [3]). One limitation of this approach is an inherent ambiguity when mapping back the information obtained from the topology of a space (say the geometric realization of a simplicial complex) to the basic elements (in this case the vertices of the simplicial complex). In this paper we overcome this problem by applying a new tool introduced in [1] – namely *Harmonic* Persistent Homology. Use of harmonic persistent homology yields an unambiguous way of selecting representative cycles from homology classes, which furthermore satisfy certain theoretical guarantees (simplices, which are essential for a class, appear with highest weight). Use of harmonic homology thus overcomes a basic obstacle for the use of TDA in the context of genomic data analysis, where identifying important simplices (which encodes biologically relevant relationships) is crucial. Although TDA and persistent homology have been applied in analyzing multi-omics data [10,20,22],

*Supported by IBM Research

†These authors contributed equally to this work

they were different in scope as they simply used persistent homology to identify broad spatial patterns in multi-omics data and were plagued by the aforementioned issue of mapping the learned topological structure back to the elements or vertices in the simplicial complex. We perform computation of persistent harmonic cycles with our software library, called `maTiLDA`, available at <https://github.com/IBM/matilda>.

Intuitively, harmonic persistent homology establishes relationships between features or observations in the data that may lead to the discovery of hidden patterns and/or novel insights owing to the capability of TDA to analyze data at different scales. Moreover, harmonic persistent homology is naturally equipped to analyze high order interactions between data points, enabling explorations beyond simple pairwise interactions by analyzing homological features in dimensions higher than one. A schematic of our framework is given in Figure 1. In this manuscript, we show how harmonic persistent homology brings to light novel relationships and deeper comprehension of biological data that can help generate new hypotheses using multi-omics data. Harmonic persistent homology has the ability to assign weights on the simplices and therefore in the feature space that it spans. These weights can be used to scale the distribution of multi-omics variables providing an additional information on importance of those variables. Due to the absence of methods and data that addresses the precise problem, it is hard to perform a benchmark comparison of the different tools reported in literature. Therefore, in this manuscript, we demonstrate the capability of harmonic persistent homology by reproducing and expanding on known results from the literature. In particular, using different datasets, such as bulk RNA from CLL patients [9], single cell RNA (scRNA) data from Richter Syndrome (RS) and CLL patients [14], and multi-omics lung adenocarcinoma (LUAD) and breast cancer (BRCA) data from The Cancer Genome Atlas (TCGA) database⁴, we validate the patterns found by our framework using external clinical knowledge and expected baseline patterns.

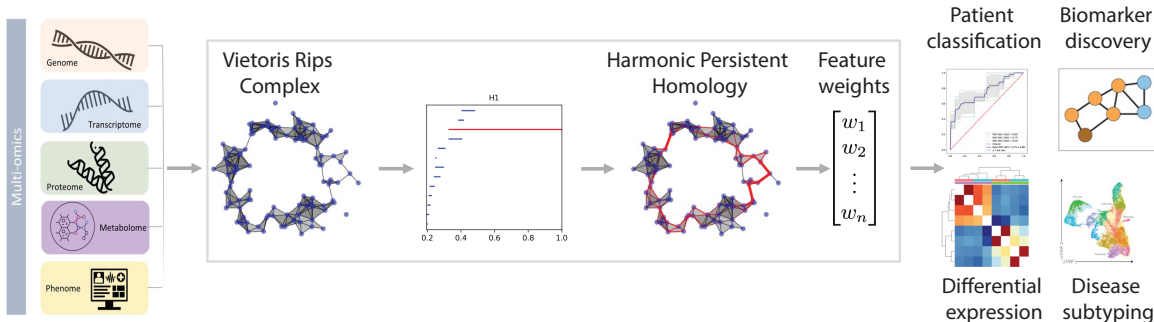


Fig. 1: Schematic of the Harmonic Framework. Given a set of multi-omic samples, the algorithm builds a topological structure on top of the input data according to a predefined similarity measure; and computes its persistent homology barcode. A subset of bars is selected from the barcode and their corresponding harmonic representatives are computed. The harmonic representative corresponding to the red bar in the diagram is depicted in red in *Harmonic Persistent Homology* panel, edges’ thickness are proportional to their harmonic weights. Harmonic weights on the simplices (e.g. edges) can then be converted to weights on the samples and used as feature vectors for a series of downstream tasks (we limit ourselves to a few examples).

Roadmap. In the next section we give the mathematical underpinnings for the essential simplices and harmonic persistent homology. In Section 3, we apply our framework to different datasets and summarize the results.

2 Methods

The goal of this section is to provide the mathematical background for our Harmonic Framework. In Section 2.1 we recall some basic definitions from simplicial homology theory. The interested reader is directed

⁴<https://www.cancer.gov/tcga>

to [7] for a more in-depth background on Topological Data Analysis. We define Harmonic Homology in Section 2.2 and introduce Harmonic Persistent Homology in Section 2.3. We explain the relation between essential simplices and the harmonic representative in Section 2.4 and provide a toy example in Figure 2j (and Section 1 in Supplementary Note). Finally, we describe how to apply this framework to real-world data in Section 2.5, with a specific use-case in Algorithm 1.

2.1 Simplicial complex and boundary maps

Definition 1. A finite simplicial complex K is a set of ordered subsets of $[N] = \{0, \dots, N\}$ for some $N \geq 0$, such that if $\sigma \in K$ and τ is a subset of σ , then $\tau \in K$.

Notation 1 If $\sigma = \{i_0, \dots, i_p\} \in K$, with K a finite simplicial complex, and $i_0 < \dots < i_p$, we will denote $\sigma = [i_0, \dots, i_p]$ and call σ a p -dimensional simplex of K . We will denote by $K^{(p)}$ the set of p -dimensional simplices of K .

Definition 2 (Chain groups and their standard bases). Suppose K is a finite simplicial complex. For $p \geq 0$, we will denote by $C_p(K) = C_p(K, \mathbb{R})$ (the p -th chain group), the \mathbb{R} -vector space generated by the elements of $K^{(p)}$, i.e.

$$C_p(K) = \bigoplus_{\sigma \in K^{(p)}} \mathbb{R} \cdot \sigma.$$

The tuple $(\sigma)_{\sigma \in K^{(p)}}$ is then a basis (called the standard basis) of $C_p(K)$ (where by a standard abuse of notation we identify σ with the image of $1 \cdot \sigma$ under the canonical injection of the direct summand $\mathbb{R} \cdot \sigma$ into $C_p(K) = \bigoplus_{\sigma \in K^{(p)}} \mathbb{R} \cdot \sigma$).

Definition 3 (The boundary map). We denote by $\partial_p(K) : C_p(K) \rightarrow C_{p-1}(K)$ the linear map (called the p -th boundary map) defined as follows. Since $(\sigma)_{\sigma \in K^{(p)}}$ is a basis of $C_p(K)$ it is enough to define the image of each $\sigma \in C_p(K)$. We define for $\sigma = [i_0, \dots, i_p] \in K^{(p)}$,

$$\partial_p(K)(\sigma) = \sum_{0 \leq j \leq p} (-)^j [i_0, \dots, \widehat{i_j}, \dots, i_p] \in C_{p-1}(K),$$

where $\widehat{\cdot}$ denotes omission.

One can easily check that the boundary maps ∂_p satisfy the key property that

$$\partial_{p+1}(K) \circ \partial_p(K) = 0,$$

or equivalently that

$$\text{Im}(\partial_{p+1}(K)) \subset \ker(\partial_p(K)).$$

Notation 2 (Cycles and boundaries) We denote

$$Z_p(K) = \ker(\partial_p(K)),$$

(the space of p -dimensional cycles) and

$$B_p(K) = \text{Im}(\partial_{p+1}(K))$$

(the space of p -dimensional boundaries).

Definition 4 (Simplicial homology groups). The p -dimensional simplicial homology group $H_p(K)$ is defined as

$$H_p(K) = Z_p(K)/B_p(K).$$

Note that $H_p(K)$ is a finite dimensional \mathbb{R} -vector space.

2.2 Representing homology classes by harmonic chains

Let K be a finite simplicial complex. We make the chain group $C_p(K)$ into an Euclidean space by fixing an inner product defined by:

$$\langle \sigma, \sigma' \rangle = \delta_{\sigma, \sigma'}, \sigma, \sigma' \in K^{(p)} \quad (1)$$

(i.e. we declare the basis $(\sigma)_{\sigma \in K^{(p)}}$ to be an orthonormal basis).

Definition 5 (Harmonic homology subspace). For $p \geq 0$, we will denote

$$\mathfrak{h}_p(K) = Z_p(K) \cap B_p(K)^\perp.$$

and call $\mathfrak{h}_p(K) \subset C_p(K)$ the harmonic homology subspace of K .

In terms of matrices, we have the following description of $\mathfrak{h}_p(K)$ as a subspace of $C_p(K)$. For $p \geq 0$, let $\mathcal{A}_p(K)$ denote an orthonormal basis of $C_p(K)$ (for example, if the chosen inner product is the standard one given in (1), then we can take $\mathcal{A}_p(K) = \{\sigma | \sigma \in K^{(p)}\}$). Let $M_p(K)$ denote the matrix of ∂_p with respect to the basis $\mathcal{A}_p(K)$ of $C_p(K)$, and the basis $\mathcal{A}_{p-1}(K)$ of $C_{p-1}(K)$. Then, $\mathfrak{h}_p(K)$ can be identified as the subspace of $C_p(K)$ which is equal to the intersection of the nullspaces of the two matrices $M_p(K)$ and $M_{p+1}(K)^T$. More precisely,

$$z \in \mathfrak{h}_p(K) \Leftrightarrow [z]_{\mathcal{A}_p(K)} \in \text{null}(M_p(K)) \cap \text{null}(M_{p+1}(K)^T). \quad (2)$$

The dimensions of the harmonic homology subspaces defined above coincide with the dimensions of the corresponding simplicial homology groups. In fact there is a well known canonically defined isomorphism between the two. We include the proof this well known fact below for completeness.

Proposition 1. The map $\mathfrak{f}_p(K)$ defined by

$$z + B_p(K) \rightarrow \text{proj}_{B_p(K)^\perp}(z), z \in Z_p(K) \quad (3)$$

gives an isomorphism $\mathfrak{f}_p(K) : \mathbb{H}_p(K) \rightarrow \mathcal{H}_p(K)$.

Proof. First observe that using the fact that $B_p(K) \subset Z_p(K)$, we have that for $z \in Z_p(K)$, $\text{proj}_{B_p(K)^\perp}(z) \in Z_p(K)$, and so the map $\mathfrak{f}_p(K)$ is well defined. The injectivity and surjectivity of $\mathfrak{f}_p(K)$ are then obvious.

The harmonic homology group $\mathcal{H}_p(K)$ is also equal to the kernel of the linear map $\Delta_p = \partial_{p+1} \circ \partial_{p+1}^* + \partial_p^* \circ \partial_p$. We omit the proof of this classical fact (see for example, [2]). The linear map $\Delta_p(K) : C_p(K) \rightarrow C_p(K)$ is a discrete analog of the Laplace operator and thus it makes sense to call its kernel the space of harmonic cycles.

2.3 Persistent Harmonic Homology

Even though the data that we deal with in this paper does not have a geometric origin, in order to visualize the concept of persistent homology it is useful to first consider the case of a point-cloud $S \subseteq \mathbb{R}^n$ that approximates some underlying manifold M . Since we only have access to S , with it we will construct an object that approximates the “shape” of M . To do this, consider n -dimensional balls of radius r centered on elements of S and denote their union by X_r . A well-known result in algebraic topology known as the *Nerve Lemma* assures us that the “shape” of the union of these balls is encoded in a simplicial complex (Definition 1) constructed using intersections of the aforementioned balls (more specifically, we consider the *nerve* of the covering formed by the balls). The choice of radius r is not clear, however, and thus we let it take all values in $[0, \infty)$ while keeping track of “shape” changes in X_r .

As one can easily visualize, as r starts growing from 0, there are many spurious homology classes that are born and quickly die off (e.g. the corresponding holes are filled in) and these have nothing to do with the topology of M . Persistent homology is a tool that can be used to separate this “noise” from the *bona fide* homology classes of M .

The mathematical notion that encapsulates these intuitions is called *Persistent Homology*. For a finite filtered simplicial complex X , that is, a sequence of finite simplicial complexes $\{X_i\}_{1 \leq i \leq n}$ with $X_i \subseteq X_j$ if $i \leq j$ taking only a finite number of different values, we define their *Persistent Homology* of degree p by

$$PH_p(X) = (\{H_p(X_i)\}_{1 \leq i \leq n}, \{\iota_*^{i,j}\}_{i,j \in \{1, \dots, n\}})$$

and their *Persistent Homology Groups* by

$$H_p^{i,j}(X) = \iota_*^{i,j}(X_p)$$

where $\iota_*^{i,j}$ is the morphism in homology induced by the inclusion $X_i \subseteq X_j$.

The structure of $PH_p(X)$ is that of a *persistence module* (which is a graded module over the graded ring of polynomials in one variable). There exists a finite multiset $D = \{(r_1, s_1), \dots, (r_l, s_l)\}$ of pairs satisfying $r_i < s_i$ that encodes the isomorphism class of $PH_p(X)$. The pairs (r_i, s_i) have interpretations as the birth-time and death-time of homology classes that appear in the various $H_p(X_i)$, and is usually called (and displayed as) the *barcode* of the filtration \mathcal{F} (the pairs (r_i, s_i) themselves are referred to as bars of the filtration).

Bars of short length corresponds to noise, while the ones which are long (persistent) reflect the homology of the underlying manifold M . The barcode of the filtration associated to S can be used as a feature of S for learning or comparison purposes. In particular, the barcodes of two finite sets S, S' , which are “close” as finite metric spaces, are themselves close under appropriately defined notion of distance between barcodes. An example of a filtration with its corresponding barcode is shown in Figure 2 (and Section 1 in Supplementary Note).

Notice that the barcode of a filtration (being just a set of ordered pairs of numbers) do not record any information about the underlying simplicial complex – in particular, about the structure and the cycles representing the homology classes whose births and deaths are encoded by the bars. Adding that information is not a trivial task. Strictly speaking homology classes representing bars are themselves elements of certain sub-quotients of vector spaces spanned by the simplices of the complex – and this introduces an inherent ambiguity in choosing representative cycles to represent bars. The authors of [1] overcome this problem by introducing an extra structure (inner product) on the vector spaces (the so called chain spaces) arising in the definition of homology – and using this inner product there is a canonical choice of cycles (called harmonic cycles) which represent the bars in the persistent bar codes.

It turns out that the harmonic bars have a certain additional property (proved in [1]) which makes them suitable choice as representatives. The harmonic bars put higher weights on simplices that are *essential* – meaning that the simplices that *must* appear with non-zero coefficient in *any* choice of representative cycle for that particular bar. This last property indicates that the weight of the simplices in harmonic representatives of the bars in a bar diagram of filtrations coming from genomic data could carry important information about biological relationships. The main goal of this paper is to understand how far this is true by applying harmonic persistence theory to multi-omics data sets and check whether it can perform certain tasks, like developing prognostic biomarker signatures in complex diseases prognosis, predicting subtypes and discovering biomarkers for accelerating therapeutic discovery.

2.4 Essential simplices and harmonic representative

Given a bar in the persistent barcode of a filtration (arising from some application) it is often natural to ask for a cycle in the cycle space of the simplicial complex representing this bar. However, such cycles are only defined modulo some equivalences – and so there is no unique answer to this question. In application (see for example [3]) it is also important to associate a set of simplices to a given bar which play the most important role in the birth of the bar. We call this set, the set of essential simplices of the bar and denote it as $\Sigma(b)$ (see [1] for a precise definition).

If b is a bar in the barcode of a filtration and z is a cycle representing b , then the set of simplices that appear with a non-zero coefficient in z contains the set of essential simplices of b , but could be larger. One measure of the “quality” of the representing cycle z is the relative weights of the essential and the non-essential simplices appearing in its support. The following quantity was defined in [1] as a measure of this quality.

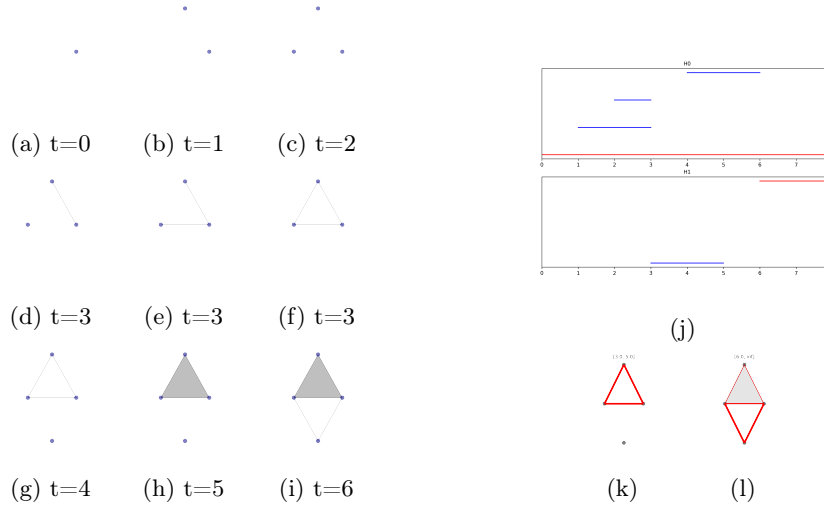


Fig. 2: Example of a filtered simplicial complex and its persistent homology, found in [1]. Figures 2a through 2i illustrate the stages of the filtration, and Figure 2j is the barcode associated to the filtration. Skeleton and barcode plots were created using `maTilda`. Figures 2k and 2l show harmonic representatives in red, with thickness proportional to the absolute value of coefficients in a chain of a given simplex.

Definition 6 (Relative essential content). Let b be a bar in the barcode of a filtration, and $z = \sum_{\sigma \in K^{(p)}} c_{\sigma} \sigma$ is a cycle representing z . We denote

$$\text{content}(z) = \left(\frac{\sum_{\sigma \in \Sigma(b)} c_{\sigma}^2}{\sum_{\sigma \in K^{(p)}} c_{\sigma}^2} \right)^{1/2}.$$

We will call $\text{content}(z)$ the relative essential content of z .

The following theorem proved in [1] and which justifies our approach in the current paper states that that the relative essential content is maximized by the harmonic representative of a bar.

Theorem 1 (Harmonic representatives maximize relative essential content). With the same notation used above, let z_0 be a harmonic representative of a bar b . Then for any cycle z representing b ,

$$\text{content}(z) \leq \text{content}(z_0).$$

Remark 1. Note that Theorem 1 implies in particular that the relative essential contents of any two harmonic representatives of a simple bar are equal. But this is clear also from the definition of the relative essential content and the fact that any two harmonic representatives of a simple bar are proportional.

2.5 Harmonic Weights from Data

We developed the following methodology to extract harmonic weights from multi-omics data, as depicted in Figure 1. Given a collection of samples together with an appropriate notion of distance (euclidean, correlation, cosine, etc.), we build the following structure on top of it and compute its persistent homology barcodes.

Definition 7 (Vietoris-Rips complex). Let X be a finite collections of points. Given a parameter $\epsilon \geq 0$, the Vietoris-Rips complex constructed from X is the collection of all subset of diameter at most 2ϵ , where the diameter is the greatest distance between any pair of vertices

$$V-R(X, \epsilon) = \{\sigma \subseteq X \mid \text{diam}(\sigma) \leq 2\epsilon\} \quad .$$

The filtration of each simplex is given by its diameter.

It should be noted that, for too large values of the parameter ϵ , the size of a Vietoris-Rips complex tends to grow exponentially with the number of points. As a matter of fact, it is straightforward to show that for any ϵ larger than the largest distance between any pairs of points; the resulting complex will be fully connected and it will contain 2^n simplices, where n is the number of data points. In order to avoid this exponential explosion, it is common practice to choose a value of ϵ strictly less than the diameter of the whole point cloud. A possible heuristic for the choice of ϵ is using the maximal distance between any point and its nearest neighbour, in order to assure the existence of only one connected component at the maximum filtration level. For the applications described in Section 3 we choose the minimal ϵ such that all 1-dimensional bars have finite length.

For a given dimension p , usually $p = 1$, we select all the bars in the p -dimensional barcode that are longer than a threshold and compute their harmonic representatives. Such threshold can be determined as a specific quantile of the distribution of the bars' lengths. As mentioned in the previous section, each p -dimensional harmonic representative consists of a linear combination of p -simplices. In particular, each 1-dimensional harmonic representative is a linear combination of edges. The absolute values of the coefficients of such linear combinations are the *harmonic weights*. Harmonic weights take value in the unit interval $[0, 1]$ and they encode how important each simplex is for a given cycle; in particular, all essential simplices have weight 1.

Since each p -dimensional simplex corresponds to a collection of $(p + 1)$ data points⁵, we can assign weights to the datapoints themselves by considering for each node in the Vietoris-Rips complex, the sum of the weights of its cofaces. For example, given a 1-dimensional harmonic representative, we can translate the weights from the edges to the nodes by assigning to each node the sum of the weights of its adjacent edges. This gives us a set of weights on the nodes for each bar.

3 Results and Discussion

In this section, we are going to showcase some possible applications of harmonic persistent homology in multi-omics data. We analyze a few public datasets with different omic profiles such as transcriptomics, DNA methylation, single cell RNAseq, as well as, drug resistance to highlight how our framework is able to capture intrinsic and hidden features in the data. In particular, Sections 3.1 and more analyses in Supplementary Note (Section 2.1 and 2.2) demonstrate when the weight of the edges are considered, while Sections 3.2 and 3.3 exemplify when the weight on the nodes are considered (as described in Section 2.5).

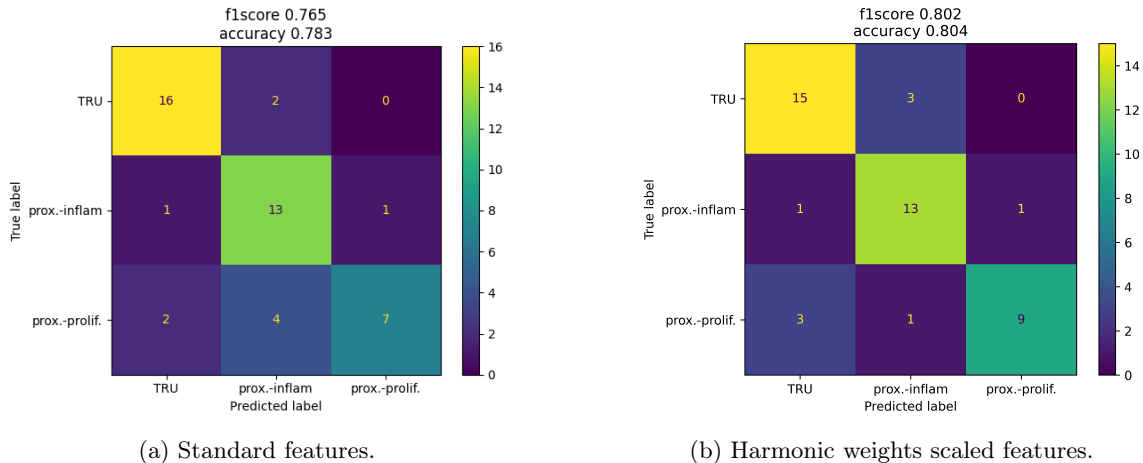


Fig. 3: Confusion matrix of the evaluation set with XGBoost classifier predicting the LUAD subtypes with the colorbar representing the number of true and false positives for each subtype.

⁵Recall that points are 0-dimensional simplices, edges are 1-dimensional, etc.

3.1 Harmonic persistent homology predicts lung cancer disease subtypes

We analyzed gene expression data of 230 samples from the Cancer Genome Atlas Lung Adenocarcinoma (TCGA-LUAD) data collection, comprising of transcriptional subtypes, such as terminal respiratory unit (TRU; $n = 89$), proximal-inflammatory (prox.-inflam; $n = 78$), and proximal-proliferative (prox.-prolif; $n = 63$). We selected $d = 5000$ out of 19,938 genes with highest variance in the expression levels and refer to them as “standard” features. We observed that the disease subtypes are clustered together when we projected the top two principal components after computing principal component analysis (PCA) on the data (Supplementary Figure 1). We then used our pipeline to enhance these features using Algorithm 1.

Algorithm 1 Disease subtype prediction with harmonic persistent homology

Require: A matrix, $A \in \mathbb{R}^{n \times d}$, n samples, d “standard” features.

Ensure: Prediction accuracy of disease subtypes

- 1: Build a Vietoris-Rips complex using d features as vertex set and correlation between their expression levels across samples.
 - 2: Compute the 1-dimensional persistence barcode up to a maximum filtration value of $\epsilon = 0.3$ (see Section 2.5).
 - 3: We sorted the bars according to their birth time and selected 30 longest bars out of 100 earliest ones
 - 4: For each one of the 30 bars, compute its harmonic representative and assign a harmonic weight to each feature (see Section 2.5).
 - 5: Obtain a single positive value for each feature by aggregating (sum) all the 30 harmonic weights for each feature.
 - 6: Rescale the original features by multiplying the expression levels of each feature by its harmonic weight.
 - 7: Split the data into training (70%) and evaluation (30%) set.
 - 8: Train various machine learning models with hyperparameter tuning and five-fold cross validation on both “standard” features and “rescaled” features using harmonic weights.
 - 9: Compute accuracy measures, such as the F_1 score, from the true positive, false positives, true negatives, and false negatives.
-

As part of the hyperparameter tuning process (Section 2.1 in Supplementary Note) in Algorithm 1, we found XGBoost [6] model to perform best on both the standard and harmonic feature sets. We observed that the F_1 score of the multiclass classification task on the three disease subtypes from the held-out evaluation set was 0.802 using the harmonic weights scaled features as compared to 0.765 using the “standard” features, which forms the baseline (Fig. 3). We repeated the training and evaluation process 40 times with different training and held-out splits in the data and observed that the median weighted F_1 score on the held-out set for the classifier trained on the standard features was 0.79, which increased to 0.81 when training on the harmonic rescaled features. We note that only 860 of the 5,000 genes have a non-zero harmonic weight, and only 196 of them resulted in a weight greater than 0.1. After selecting the top 20 genes sorted by their harmonic weights and performing gene set enrichment analysis we observed that adenocarcinoma of lung cancer was found as the target disease ($p < 10^{-4}$), pathways such as *cellular macromolecule metabolic process* ($p < 10^{-3}$), *structural constituent of ribosome* function ($p < 10^{-2}$) were found to be significant, among others. Genes such as VSIG4, DOK2, MS4A4A, CKAP5 had the highest associated harmonic weight, beyond ribosomal protein housekeeping genes such as RPS5, RPL27, etc. All of these genes are known to be associated with lung cancer [4,11,23] The predictive power for lung adenocarcinoma subtypes along with interpretability of genes associated with the disease with their weights as a metric of importance leads to the interpretability of standard features and a paradigm for feature selection using harmonic weights, and renders this harmonic pipeline useful for high dimensional multi-omics datasets.

3.2 Discovering breast cancer subtypes in multi-omics data

To showcase how harmonic persistent homology can be used in multi-omics analyses, we analyzed a set of 690 breast cancer samples from the TCGA database for which both RNAseq and Methylation450 data are present. The dataset is comprised of 414 Luminal-A, 141 Luminal-B, and 135 basal-like samples, and we considered 28,495 genes and 363,791 methylation sites for a total of 392,286 features. We concatenated the RNAseq and Methylation450 data and projected them to a 100-dimensional space using PCA. We built a

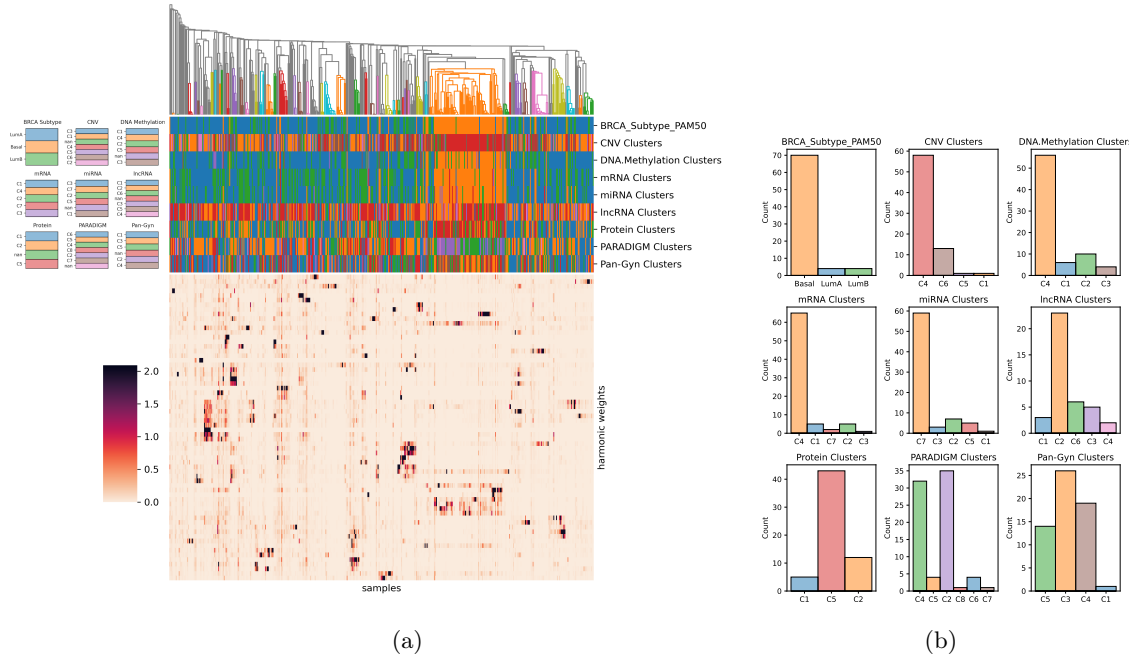


Fig. 4: Single-linkage hierarchical clustering of breast cancer samples using harmonic weights is able to detect a large basal-like cluster, depicted in orange in (a). The distributions of different descriptors for samples in this cluster are shown in (b). The color scheme for each descriptor is consistent across the two panels.

Vietoris-Rips complex using distance correlation and computed its 1-dimensional persistent homology up to a maximum filtration value of 0.75. We then computed the harmonic representatives of all 66 bars longer than 0.07 (0.97 quantile). For each representative we extracted the harmonic weights on the samples, resulting in a 690×66 weights matrix, depicted in Figure 4a. Single-linkage clustering on the samples' weights revealed a large cluster of mostly basal-like samples, whose characteristic are shown in Figure 4b. It is important to note that this cluster was found using harmonic persistent homology on samples in an unsupervised manner, without any knowledge of the nine descriptors shown on top of Figure 4a. The clusters can be used to externally validate our findings and show how different harmonic cycles capture interactions between different subsets of data as the cycles with similar weights cluster together samples with similar descriptors. This approach can be extended to other multi-omics data, leading to a nuanced, data-driven discovery of novel subgroups of patients along with their associated biomarkers.

3.3 Transcriptomic discovery associated with treatment progression

We consider transcriptomic data of 11 CLL patients that were treated with Venetoclax (a BCL2 inhibitor) as discussed in [9] and for which RNA data were collected pre-treatment and post-treatment during which the patient disease was progressing. We selected 98 genes that are known to be associated to CLL (see Supplementary Section 3 for the full list) and provided as input to our harmonic framework the pre- and post-treatment cohorts independently. Harmonic persistent homology identified relevant genes in each of the two cohorts as those genes with non-zero harmonic weights, and we performed a STRING DB network [17] analysis (see Fig 5) to analyze protein-protein interactions of the identified genes. At pre-treatment time-points, there was significant enrichment of genes in the apoptosis (strength 0.83, FDR 1.9e-04, pink) and regulation of cell differentiation pathways (strength 0.87, FDR 4.28e-05, yellow). In the post-treatment, progression time point, we see significant enrichment in BCR signaling (strength 1.87, FDR 2.58e-12, red) and MAPK signaling (strength 1.31, FDR 7.00e-05, purple) involving the genes *BTK*, *MAPK1*, *KRAS*, and *NRAS*. Upregulation of BCR signaling has been associated with Venetoclax progression with activation of the downstream MAPK signaling pathways [9,18]. Furthermore, there was also enrichment of NF- κ B signaling pathways, which included the genes *TRAF3* and *NFKBIE* (strength 1.44, FDR 8.7e-4, yellow), and

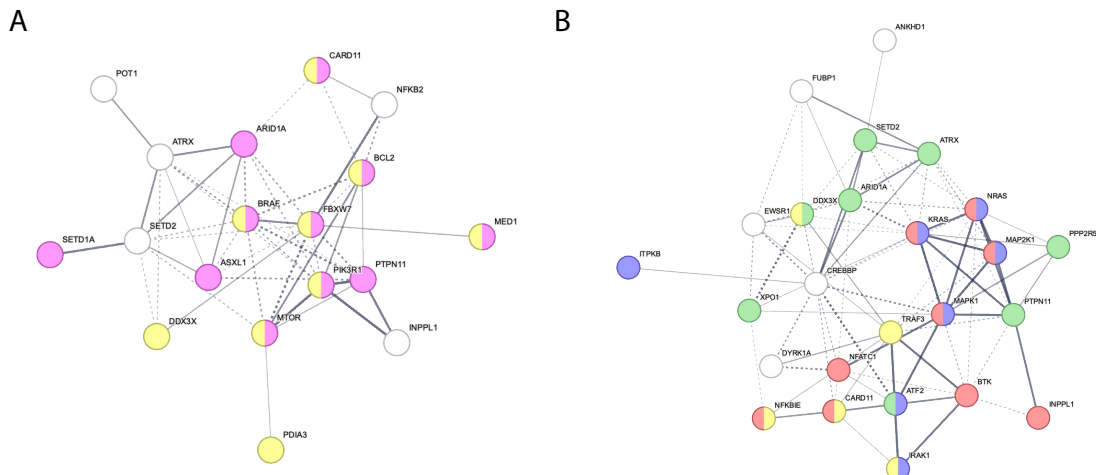


Fig. 5: STRING network of the harmonic persistent homology identified genes. The edges indicate both functional and physical association. Edge thickness indicates strength of support for the edge (thick solid: >80% of samples, thin solid: >60%, dashed: >40% support). A: Genes set for the pre-treatment cohort; nodes in pink belong to the Regulation of cell differentiation strength, while the one in yellow to the Reg. apoptotic process. B: Gene set for the post-treatment cohort; node belonging to MAPK cascade are in purple, Reg. of cell in green, Toll like receptor cascades, and NFKappa B sig. in yellow and BCR pathway in red.

regulation of cell cycle (strength 0.85, FDR 0.0058, green). These results demonstrate the ability of our harmonic framework to extract clinically/biological plausible gene sets supported by the existing literature [9,18] and whose clinical findings offer a measure of validation. It is worthy to note here that standard machine learning methods are not best suited to analyze this data, given the small sample size, which is often the case in various cancer datasets. However, harmonic persistent homology is capable to find previously validated and novel signals in such datasets where the sample size is very low, paving the path for efficient biomarker discovery.

4 Conclusion

Here we utilize the fact that harmonic cycles maximize the contribution of essential simplices, and this paper is the first application of harmonic persistent homology to biological problems. We introduce a framework that uses harmonic persistent homology to extract information from multi-omics data that enables the discovery of hidden structures in data that have the potential to inform clinical questions. Harmonic persistent homology overcomes a challenge in TDA by enabling us to systematically map the topological features uniquely to the input data and additionally, the associated weights capture the importance of the biological markers. It does so even when the data size is small, as we see in one of the applications. We applied harmonic persistent homology in a variety of scenarios in cancer with distinct questions such as subtype prediction, unsupervised subtype detection and biomarker discovery in multi-omics data. In lung cancer, we showed that, harmonic weight rescaled features improved disease subtype prediction accuracy as compared to the baseline; in breast cancer we used harmonic weights on samples to discover a basal-like cluster; and in Venetoclax treatment response dataset, we discovered biologically relevant genes just with 11 samples. In conclusion, harmonic persistent homology has the potential of therapeutic implications for complex diseases, extending the breadth of applications of TDA in biological and healthcare data.

5 Author Contributions

L.P, S.B, and A.G.S conceived this project. D.G and A.G.S implemented the harmonic persistent homology. F.U and A.B conceived the experiments and performed data quality control. All authors discussed results and wrote the manuscript.

6 Competing Interests

D.G., L.P., A.G.S., F.U. and A.B. are listed (together or partially) as co-inventor of 18/506194, 18/506187, 18/616298 patent applications currently pending review at the USPTO related to the Harmonic applications.

7 Acknowledgements

SB was partially supported by NSF grants CCF-1910441 and CCF-2128702. We are very grateful to Aishath Naeem for her insight in interpreting the CLL patient results, and Kahn Rhrissorrakrai for reviewing the manuscript and providing insightful comments. DG performed this work during an internship at IBM Research. The results shown here are in whole or part based upon data generated by the TCGA Research Network: <https://www.cancer.gov/tcga>.

8 Availability and Implementation

Source code, user manual, and sample input-output sets are available for downloading at <https://github.com/IBM/matilda>.

References

1. Basu, S., Cox, N.: Harmonic persistent homology (extended abstract). In: 2021 IEEE 62nd Annual Symposium on Foundations of Computer Science—FOCS 2021, pp. 1112–1123. IEEE Computer Soc., Los Alamitos, CA ([2022] ©2022). <https://doi.org/10.1109/FOCS52979.2021.00110>, <https://doi.org/10.1109/FOCS52979.2021.00110>
2. Basu, S., Cox, N.: Harmonic persistent homology. *SIAM Journal on Applied Algebra and Geometry* **8**(1), 189–224 (2024). <https://doi.org/10.1137/22M1518761>, <https://epubs.siam.org/doi/abs/10.1137/22M1518761>
3. Basu, S., Utro, F., Parida, L.: Essential Simplices in Persistent Homology and Subtle Admixture Detection. In: Parida, L., Ukkonen, E. (eds.) 18th International Workshop on Algorithms in Bioinformatics (WABI 2018). *Leibniz International Proceedings in Informatics (LIPIcs)*, vol. 113, pp. 14:1–14:10. Schloss Dagstuhl–Leibniz-Zentrum fuer Informatik, Dagstuhl, Germany (2018). <https://doi.org/10.4230/LIPIcs.WABI.2018.14>, <http://drops.dagstuhl.de/opus/volltexte/2018/9316>
4. Berger, A.H., Chen, M., Morotti, A., Janas, J.A., Niki, M., Bronson, R.T., Taylor, B.S., Ladanyi, M., Van Aelst, L., Politi, K., et al.: Dok2 inhibits egfr-mutated lung adenocarcinoma. *PLoS One* **8**(11), e79526 (2013)
5. Bose, A., Platt, D.E., Haiminen, N., Parida, L.: Cuna: Cumulant-based network analysis of genotype-phenotype associations in parkinson’s disease. *medRxiv* (2021). <https://doi.org/10.1101/2021.08.02.21261457>, <https://www.medrxiv.org/content/early/2021/08/05/2021.08.02.21261457>
6. Chen, T., Guestrin, C.: Xgboost: A scalable tree boosting system. In: *Proceedings of the 22nd ACM SIGKDD International Conference on Knowledge Discovery and Data Mining*. p. 785–794. KDD ’16, Association for Computing Machinery, New York, NY, USA (2016). <https://doi.org/10.1145/2939672.2939785>, <https://doi.org/10.1145/2939672.2939785>
7. Edelsbrunner, H., Harer, J.L.: *Computational topology: an introduction*. American Mathematical Society (2022)
8. Hasin, Y., Seldin, M., Lusis, A.: Multi-omics approaches to disease. *Genome biology* **18**(1), 1–15 (2017)
9. Khalsa, J.K., Cha, J., Utro, F., Naem, A., Murali, I., Kuang, Y., Vasquez, K., Li, L., Tyekucheva, S., Fernandes, S.M., Veronese, L., Guieze, R., Sasi, B.K., Wang, Z., Machado, J.H., Bai, H., Alasfour, M., Rhrissorakrai, K., Levovitz, C., Danysh, B.P., Slowik, K., Jacobs, R.A., Davids, M.S., Paweletz, C.P., Leshchiner, I., Parida, L., Getz, G., Brown, J.R.: Genetic events associated with venetoclax resistance in CLL identified by whole-exome sequencing of patient samples. *Blood* **142**(5), 421–433 (08 2023). <https://doi.org/10.1182/blood.2022016600>, <https://doi.org/10.1182/blood.2022016600>
10. Liao, T., Wei, Y., Luo, M., Zhao, G.P., Zhou, H.: tmap: an integrative framework based on topological data analysis for population-scale microbiome stratification and association studies. *Genome biology* **20**, 1–19 (2019)
11. Liao, Y., Guo, S., Chen, Y., Cao, D., Xu, H., Yang, C., Fei, L., Ni, B., Ruan, Z.: Vsig4 expression on macrophages facilitates lung cancer development. *Laboratory investigation* **94**(7), 706–715 (2014)
12. Libbrecht, M.W., Noble, W.S.: Machine learning applications in genetics and genomics. *Nature Reviews Genetics* **16**(6), 321–332 (2015)
13. McGuirl, M.R., Volkening, A., Sandstede, B.: Topological data analysis of zebrafish patterns. *Proceedings of the National Academy of Sciences* **117**(10), 5113–5124 (2020)
14. Parry, E.M., Leshchiner, I., Guièze, R., Johnson, C., Tausch, E., Parikh, S.A., Lemvigh, C., Broséus, J., Hergalant, S., Messer, C., Utro, F., Levovitz, C., Rhrissorakrai, K., Li, L., Rosebrock, D., Yin, S., Deng, S., Slowik, K., Jacobs, R., Huang, T., Li, S., Fell, G., Redd, R., Lin, Z., Knisbacher, B.A., Livitz, D., Schneider, C., Ruthen, N., Elagina, L., Taylor-Weiner, A., Persaud, B., Martinez, A., Fernandes, S.M., Purroy, N., Anandappa, A.J., Ma, J., Hess, J., Rassenti, L.Z., Kipps, T.J., Jain, N., Wierda, W., Cymbalista, F., Feugier, P., Kay, N.E., Livak, K.J., Danysh, B.P., Stewart, C., Neuberg, D., Davids, M.S., Brown, J.R., Parida, L., Stilgenbauer, S., Getz, G., Wu, C.J.: Evolutionary history of transformation from chronic lymphocytic leukemia to richter syndrome. *Nat. Med.* **29**(1), 158–169 (Jan 2023)
15. Platt, D., Bose, A., Levovitz, C., Rhrissorakrai, K., Parida, L.: Epidemiological topology data analysis links severe covid-19 to raas and hyperlipidemia associated metabolic syndrome conditions. *medRxiv* (2022). <https://doi.org/10.1101/2022.03.31.22273239>, <https://www.medrxiv.org/content/early/2022/04/03/2022.03.31.22273239>
16. Platt, D.E., Basu, S., Zalloua, P.A., Parida, L.: Characterizing redescription using persistent homology to isolate genetic pathways contributing to pathogenesis. *BMC Systems Biology* **10**(1), S10 (Jan 2016). <https://doi.org/10.1186/s12918-015-0251-2>
17. Szklarczyk, D., Gable, A.L., Nastou, K.C., Lyon, D., Kirsch, R., Pyysalo, S., Doncheva, N.T., Legeay, M., Fang, T., Bork, P., Jensen, L.J., von Mering, C.: The STRING database in 2021: customizable protein–protein networks, and functional characterization of user-uploaded gene/measurement sets. *Nucleic Acids Res.* **49**(D1), D605–D612 (Jan 2021)
18. Thompson, P.A., Wierda, W.G.: Eliminating minimal residual disease as a therapeutic end point: working toward cure for patients with CLL. *Blood* **127**(3), 279–286 (01 2016). <https://doi.org/10.1182/blood-2015-08-634816>, <https://doi.org/10.1182/blood-2015-08-634816>

19. Topaz, C.M., Ziegelmeier, L., Halverson, T.: Topological data analysis of biological aggregation models. *PLOS ONE* **10**(5), 1–26 (05 2015)
20. Vipond, O., Bull, J.A., Macklin, P.S., Tillmann, U., Pugh, C.W., Byrne, H.M., Harrington, H.A.: Multiparameter persistent homology landscapes identify immune cell spatial patterns in tumors. *Proceedings of the National Academy of Sciences* **118**(41), e2102166118 (2021)
21. Xia, K., Wei, G.W.: Persistent homology analysis of protein structure, flexibility, and folding. *International journal for numerical methods in biomedical engineering* **30**(8), 814–844 (2014)
22. Zheng, F., Zhang, S., Churas, C., Pratt, D., Bahar, I., Ideker, T.: Hidedf: identifying persistent structures in multiscale ‘omics data. *Genome biology* **22**(1), 1–15 (2021)
23. Zheng, Z., Li, H., Yang, R., Guo, H.: Role of the membrane-spanning 4a gene family in lung adenocarcinoma. *Frontiers in Genetics* **14**, 1162787 (2023)